

## Experimental millimeter-wave 3D woodpile EBG waveguide manufactured by layer-by-layer dicing of silicon wafers

G. Torrisi<sup>(1)</sup>, G. S. Mauro<sup>(1)(2)</sup>, A. Locatelli<sup>(3)</sup>, L. Celona<sup>(1)</sup>, C. De Angelis<sup>(3)</sup>, G. Sorbello<sup>(4)(1)</sup>

(1) Istituto Nazionale di Fisica Nucleare - Laboratori Nazionali del Sud (INFN-LNS),  
Via S. Sofia 62, 95123 Catania

(2) Dipartimento di Ingegneria dell'Informazione, delle Infrastrutture e dell'Energia Sostenibile,  
Università degli Studi Mediterranea di Reggio Calabria Salita Melissari, 89124 Reggio Calabria RC

(3) Dipartimento di Ingegneria dell'informazione, Università di Brescia, via Branze 38, 25123 Brescia (Italy)

(4) Dipartimento di Ingegneria Elettrica, Elettronica e Informatica, Università degli Studi di Catania,  
Viale Andrea Doria 6, 95125, Catania, Italia

### Abstract

In this paper we report on the design, fabrication and measurement of a silicon woodpile waveguide operating in the millimeter-wave band. The 3D Electromagnetic Band Gap (EBG) woodpile has been created by precision dicing saws of silicon wafers. An appropriate air defect has been inserted at the structure central coordinates and optimized in size and shape in order to maximize the coupling between the TE<sub>10</sub> mode of the standard rectangular Input/Output metallic waveguides and the TE<sub>10</sub>-like mode of the EBG waveguide that propagates along the defect. The manufactured device, that includes custom metal-dielectric I/O transitions, exhibits an overall  $|S_{11}|$  and  $|S_{12}|$  scattering parameters of  $-32$  dB and  $-0.46$  dB at the operating frequency of 96.6 GHz, which are in very good agreement with the simulated ones, obtained in Ansys HFSS.

### 1 Introduction

EBG structures are periodic arrangement of dielectric or metallic elements that exhibit a “bandgap” of frequencies where electromagnetic propagation is forbidden. EBG technologies at millimeter-wave frequencies can have several applications [1, 2, 3] such as antennas [4], particle acceleration [5], metamaterial and compact microwave components [6]. On the contrary of 1D [7] and 2D [8] Photonic Crystals (PhCs), three-dimensional EBG structures are able to provide a complete confinement in all directions. In this paper we present a dielectric (silicon) woodpile waveguide that provides full 3D confinement and that can be easily connected with standard metal waveguides. The woodpile (layer-by-layer) structure proposed in this paper, shown in Fig. 1, consists of stacked grating of bricks, arranged orthogonally with respect to the adjacent ones and shifted by one-half of a period ( $d/2$ ). The PhC woodpile (Fig. 1) is formed by stacking eight tiles, each of them is made by two levels of perpendicular bars and is a monolithic piece since it has been created starting from one  $2h$ -thick silicon wafer. The EBG woodpile waveguide exploits a guiding air

defect whose design is described in Section 2. For the manufacturing of the 3D EBG waveguide structure - described in Section 3 - we employed a low-cost and high precision technique based on high speed dicing saw [9, 10, 11] able to cut the silicon layers (refractive index  $n_{\text{HR-Si}} = 3.32$ ) with a very low surface roughness. Finally, in the experimental Section 4 we demonstrate that our woodpile waveguide supports a well confined TE<sub>10</sub>-like propagating mode at the frequency of about 96 GHz.

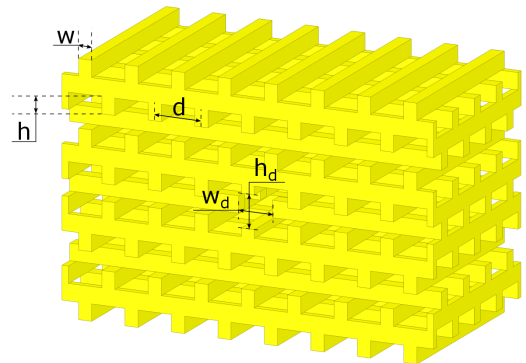


**Figure 1.** Perspective view of the woodpile waveguide with its parameters: width  $w = 0.334$  mm, height  $h = 0.425$  mm, period  $d = 1.2$  mm. The air defect of dimensions  $w_d = 0.877$  mm,  $h_d = 0.850$  mm is also visible at the center of the structure. For the experimental tests, the silicon ( $\epsilon_r = 11$ ) woodpile has been inserted into a copper box (not shown in this figure) which hosts the input/output WR10 waveguide standard flange holes.

A copper structure has also been designed and high-precision-manufactured to allow the structure alignment and the integration of input/output metallic WR10 waveguides.

### 2 EBG Woodpile Waveguide

The first step in the design of the woodpile structure for millimeter-wave frequencies is the determination of opti-

mal brick width ( $w$ ) and height ( $h$ ) to maximize the frequency bandgap. The MIT Photonic-Bands (MPB) package [12] has been used in order to determinate the optimal brick width ( $w = 0.334$  mm) and height ( $h = 0.425$  mm) and to maximize the frequency bandgap. The operating frequency of 96.6 GHz can be obtained through the evaluation of the structure period, in our case equal to  $d = 1.2$  mm. The lateral ( $xy$ ) extension has been fixed to seven periods ( $7d$ ) while the crystal height is  $15h$  to ensure low leakage [13]. Finally a rectangular defect of dimension  $w_d = 0.877$  mm  $\times$   $h_d = 0.850$  mm, with dimensions compatible with the WR10 waveguide, has been inserted at the silicon structure center in order to obtain the dielectric waveguide (see Fig. 1). The length of the device along the defect direction has been chosen equal to four periods ( $\simeq 4.8$  mm). The guided mode that propagates along the defect at the frequency of 96.6 GHz is represented by the red curve of the woodpile structure projected band diagram, visible in Fig. 2. The other two blue curves inside the band-gap are dispersion curves of two modes supported by the hollow core EBG structure cross-polarized with respect to the exciting TE<sub>10</sub> mode. The proposed metallic waveguide-to-woodpile

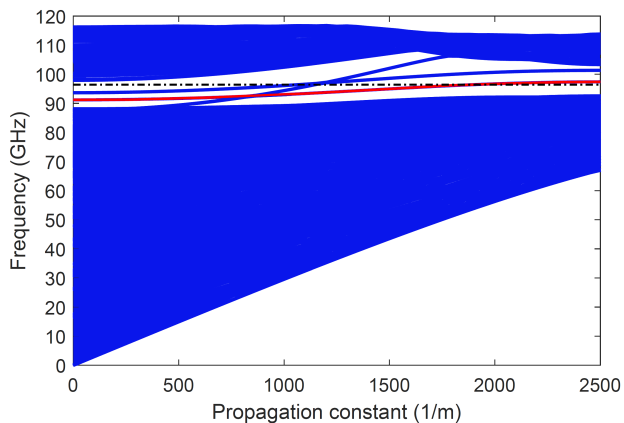


**Figure 2.** Projected band diagram of the silicon woodpile structure.

transition consists of metallic waveguides in WR10 standard juxtaposed to the dielectric woodpile waveguide input/output interfaces. This feeding scheme takes advantage from the fact that the fundamental mode of the rectangular waveguide and the woodpile waveguide mode exhibit a good modal overlap [14]: thanks to this characteristic the coupling is simpler with respect to other feeding schemes adopted in literature such as horn antennas [15] or metal waveguide inserted into the dielectric woodpile [9], where due to larger dimensions of the waveguide defect, many modes are supported by the hollow core waveguide and unwanted high order modes could be coupled. The complete 3D EBG waveguide structure, including the feeding metallic waveguides, has been simulated in HFSS [16]: the resulting electric field strength along the defect propagation direction ( $xz$  plane) is visible in Fig 3.

A silicon prototype has been realized and experimentally

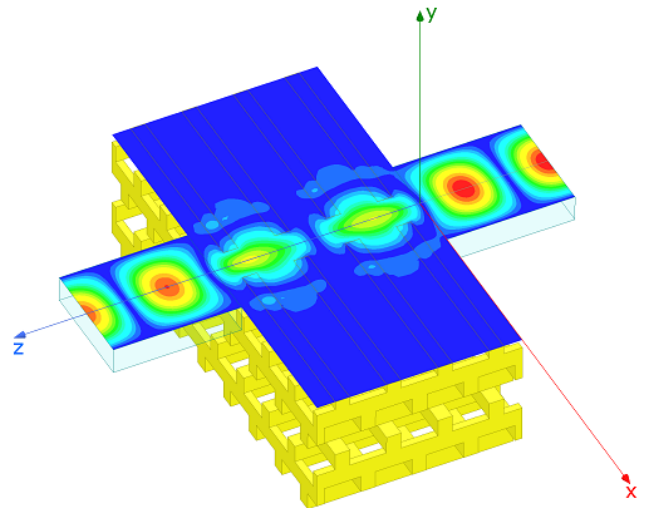


**Figure 3.** View of the simulated electric field strength at the central  $xz$  plane slice: the TE<sub>10</sub> mode from the input rectangular waveguide excites the mode inside the woodpile defect.

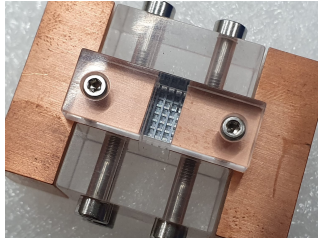
characterized as described hereinafter.

### 3 Fabrication

The proposed EBG woodpile waveguide has been manufactured at the CNR-IMM fabrication facility of Bologna by using of a high speed and precision dicing saws (geometrical tolerance of  $10 \mu\text{m}$ ). The required dimensional tolerances have been retrieved thanks to sensitivity simulations where the effects of a misalignment between the silicon device and its copper cover has been investigated. When the misalignment entity exceeds  $400 \mu\text{m}$ , the Insertion Loss (IL) 0.5 dB percentage bandwidth (%BW) decreases from the initial value of 1.9%BW (no misalignment) up to 0.7%BW with a misalignment of  $700 \mu\text{m}$ . Each silicon layer has been cutted starting from  $n$ -type FZ DSP silicon wafers  $850 \mu\text{m}$  thick, with resistivity  $> 3 \text{ k}\Omega\text{cm}$ , low effective loss tangent and high permittivity at mm-wave range [10]. The resulting bricks exhibit good sharpness and a surface roughness smaller than  $10 \mu\text{m}$ . In order align the dielectric tiles, an Oxygen Free High conductivity Copper block, including also the metallic input and output waveguides, has been realized by Wire Electrical Discharge Machining (WEDM) ( $< \pm 5 \mu\text{m}$  of tolerance). This allowed to achieve high accuracy of the final assembled device, shown in Fig. 4,

### 4 Experimental results

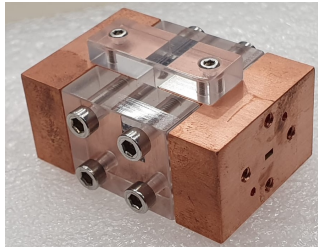
In this section, the scattering parameters obtained by 3D electromagnetic computations performed with HFSS are compared with vector network analyzer S-parameters measurement: the manufactured woodpile waveguide has been connected to mm-wave extension heads and the scattering parameter have been recorded from 95 to 98 GHz, with a



(a)



(b)



(c)

**Figure 4.** Manufactured dielectric EBG woodpile structure in top-perspective (a) and side-view (b): the eight tiles composing the woodpile have been manually inserted into the copper box. In (c) it is possible to see the waveguide WR10 port and interface with flange holes for the connection of the mm-wave extender to VNA.

frequency sample interval of 12.5 MHz. S-parameter measurements are shown in Fig. 5: at the central frequency of 96.6 GHz the  $|S_{11}|$  and  $|S_{12}|$  values are equal to  $-32$  dB and  $-0.46$  dB respectively. The measured and simulated values  $|S_{11}|$  and  $|S_{12}|$  of the dielectric woodpile, including the metallic WR10 waveguides, have been compared showing a good agreement with each other. Manufacturing tolerances

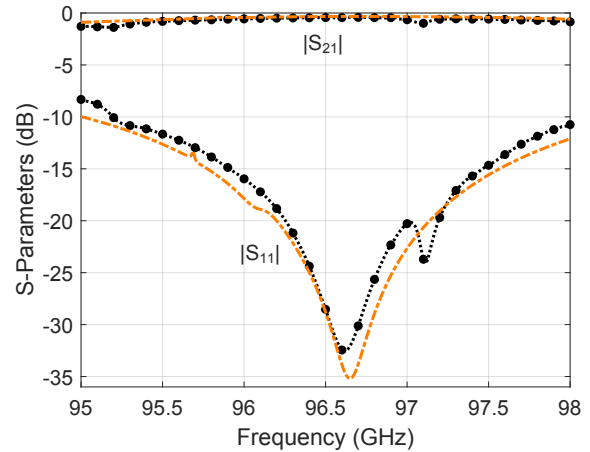


**Figure 5.** Simulated (orange dash-dotted curves) vs. experimental (black marked curves) S-parameters of the presented structure.

caused a small frequency shift additional losses could be ascribed to leakage and scattering caused by manufacturing imperfections.

## 5 Conclusion

A millimetre-wave dielectric EBG woodpile waveguide that employs a simple interface towards standard WR10 metallic waveguide has been proposed. The band-gap of the woodpile periodic structure has been optimized and the dispersion relation of the infinite periodic dielectric structure has been computed with the MIT Photonic Bands (MPB) code. The overall structure has been designed by means of full-wave 3D simulators. Dicing saws have been used to cut silicon wafers which are tile-by-tile stacked to compose the woodpile. Finally, a prototype has been realized and experimentally validated: obtained results are in very good agreement with the simulations and confirm the accuracy of the manufacturing.

## Acknowledgment

The authors would like to acknowledge the INFN V National Committee under the DEMETRA grant, the IMM (Institute of Microelectronics and Microsystems) of CNR, Bologna and the Andalò Gianni Srl”, Precision Mechanical company.

## References

- [1] J. D. Joannopoulos, S. G. Johnson, J. N. Winn, and R. D. Meade, "Photonic crystals: Molding the flow of light (second edition)," 2011.
- [2] Y. J. Lee, J. Yeo, K. D. Ko, R. Mittra, Y. Lee, and W. S. Park, "A novel design technique for control of defect frequencies of an electromagnetic bandgap (EBG) superstrate for dual-band directivity enhancement," *Microwave Opt. Technol. Lett.*, vol. 42, no. 1, pp. 25–31, 2004.
- [3] A. R. Weily, L. Horvath, K. P. Esselle, B. C. Sanders, and T. S. Bird, "A planar resonator antenna based on a woodpile EBG material," *IEEE Trans. Antennas Propag.*, vol. 53, no. 1, pp. 216–223, Jan 2005.
- [4] F. Frezza, L. Pajewski, E. Piuze, C. Ponti, and G. Schettini, "Radiation-enhancement properties of an X-band woodpile EBG and its application to a planar antenna," *Int. J. Antenn. Propag.*, vol. 2014, 2014.
- [5] G. Torrisi, L. Celona, C. De Angelis, S. Gammino, A. Locatelli, D. Mascali, G. Mauro, and G. Sorbello, "Numerical study of photonic-crystal-based dielectric accelerators," in *10th Int. Particle Acc. Conf. (IPAC'19), Melbourne, Australia, 19-24 May 2019*. JACOW Publishing, Geneva, Switzerland, 2019, pp. 3653–3656.
- [6] A. R. Weily, K. P. Esselle, T. S. Bird, and B. C. Sanders, "Experimental woodpile EBG waveguides, bends and power dividers at microwave frequencies," *Electron. Lett.*, vol. 42, no. 1, pp. 32–3–, 2006.
- [7] A. S. Jugessur, P. Pottier, and R. M. De La Rue, "One-dimensional periodic photonic crystal microcavity filters with transition mode-matching features, embedded in ridge waveguides," *Electron. Lett.*, vol. 39, no. 4, pp. 367–369, Feb 2003.
- [8] A. Locatelli, G. Sorbello, G. Torrisi, L. Celona, and C. De Angelis, "Photonic crystal waveguides for particle acceleration," in *2017 Prog. Electromagnetic Res. Symposium-Spring (PIERS)*. IEEE, 2017, pp. 1008–1013.
- [9] I. Ederra, I. Khromova, R. Gonzalo, N. Delhote, D. Baillargeat, A. Murk, B. E. J. Alderman, and P. de Maagt, "Electromagnetic-bandgap waveguide for the millimeter range," *IEEE Trans. Microw. Theory Tech.*, vol. 58, no. 7, pp. 1734–1741, 2010.
- [10] P. H. Bolivar, M. Brucherseifer, J. G. Rivas, R. Gonzalo, I. Ederra, A. L. Reynolds, M. Holker, and P. de Maagt, "Measurement of the dielectric constant and loss tangent of high dielectric-constant materials at terahertz frequencies," *IEEE Trans. Microw. Theory Tech.*, vol. 51, no. 4, pp. 1062–1066, April 2003.
- [11] *Advanced RF MEMS*, ser. The Cambridge RF and Microwave Engineering Series. Cambridge University Press, 2010.
- [12] S. G. Johnson, "MIT photonics-bands (MPB). available at <http://ab-initio.mit.edu/photons/tutorial/>."
- [13] G. S. Mauro, A. Locatelli, G. Torrisi, L. Celona, C. De Angelis, and G. Sorbello, "Woodpile EBG waveguide as a DC electrical break for microwave ion sources," *Microwave Opt Technol Lett*, 2018.
- [14] G. Torrisi, G. Sorbello, O. Leonardi, L. Celona, S. Gammino, G. Mauro, G. Castorina, B. Spataro, and V. Dolgashev, "Closed-to-open conversion of a mm-wave gaussian horn antenna," in *2018 12th EUCAP*, 2018.
- [15] C. Sell, C. Christensen, J. Muehlmeier, G. Tuttle, Z.-Y. Li, and K.-M. Ho, "Integrated horns for improved side coupling into in-plane three-dimensional photonic crystal waveguides," *Appl. Phys. Lett.*, vol. 85, no. 5, pp. 707–709, 2004.
- [16] Ansys HFSS, "Ansoft corp., Pittsburgh, PA," 2018.